

Żabińskiite, ideally $\text{Ca}(\text{Al}_{0.5}\text{Ta}_{0.5})(\text{SiO}_4)\text{O}$, a new mineral of the titanite group from the Piława Górna pegmatite, the Góry Sowie Block, southwestern Poland

ADAM PIECZKA^{1,*}, FRANK C. HAWTHORNE², CHI MA³, GEORGE R. ROSSMAN³, ELIGIUSZ SZEŁĘG⁴, ADAM SZUSZKIEWICZ⁵, KRZYSZTOF TURNIAK⁵, KRZYSZTOF NEJBERT⁶, SŁAWOMIR S. ILNICKI⁶, PHILIPPE BUFFAT⁷ AND BOGDAN RUTKOWSKI⁷

¹ AGH University of Science and Technology, Department of Mineralogy, Petrography and Geochemistry, 30-059 Kraków, Mickiewicza 30, Poland

² Department of Geological Sciences, University of Manitoba, Winnipeg, Manitoba R3T 2N2, Canada

³ Division of Geological and Planetary Sciences, California Institute of Technology, Pasadena, 91125-2500, California, USA

⁴ University of Silesia, Faculty of Earth Sciences, Department of Geochemistry, Mineralogy and Petrography, 41-200 Sosnowiec, Będzińska 60, Poland

⁵ University of Wrocław, Institute of Geological Sciences, 50-204 Wrocław, M. Borna 9, Poland

⁶ University of Warsaw, Faculty of Geology, Institute of Geochemistry, Mineralogy and Petrology, 02-089 Warszawa, Żwirki and Wigury 93, Poland

⁷ AGH University of Science and Technology, International Centre of Electron Microscopy for Materials Science, Department of Physical and Powder Metallurgy, 30-059 Kraków, Mickiewicza 30, Poland

[Received 7 January 2016; Accepted 21 April 2016; Associate Editor: Ed Grew]

ABSTRACT

Żabińskiite, ideally $\text{Ca}(\text{Al}_{0.5}\text{Ta}_{0.5})(\text{SiO}_4)\text{O}$, was found in a Variscan granitic pegmatite at Piława Górna, Lower Silesia, SW Poland. The mineral occurs along with (Al,Ta,Nb)- and (Al,F)-bearing titanites, a pyrochlore-supergroup mineral and a K-mica in compositionally inhomogeneous aggregates, $\sim 120\ \mu\text{m} \times 70\ \mu\text{m}$ in size, in a fractured crystal of zircon intergrown with polycrase-(Y) and euxenite-(Y). Żabińskiite is transparent, brittle, brownish, with a white streak, vitreous lustre and a Mohs hardness of ~ 5 . The calculated density for the refined crystal is equal to $3.897\ \text{g cm}^{-3}$, but depends strongly on composition. The mineral is non-pleochroic, biaxial (–), with mean refractive indices ≥ 1.89 . The (Al,Ta,Nb)-richest żabińskiite crystal, $(\text{Ca}_{0.980}\text{Na}_{0.015})_{\Sigma=0.995}(\text{Al}_{0.340}\text{Fe}_{0.029}^{3+}\text{Ti}_{0.298}\text{V}_{0.001}\text{Zr}_{0.001}\text{Sn}_{0.005}\text{Ta}_{0.251}\text{Nb}_{0.081})_{\Sigma=1.005}[(\text{Si}_{0.988}\text{Al}_{0.012})\text{O}_{4.946}\text{F}_{0.047}(\text{OH})_{0.007}]_{\Sigma=5.000}$; 60.7 mol.% $\text{Ca}[\text{Al}_{0.5}(\text{Ta,Nb})_{0.5}](\text{SiO}_4)\text{O}$; is close in composition to previously described synthetic material. Żabińskiite is triclinic (space group symmetry $A\bar{1}$) and has unit-cell parameters $a = 7.031(2)\ \text{\AA}$, $b = 8.692(2)\ \text{\AA}$, $c = 6.561(2)\ \text{\AA}$, $\alpha = 89.712(11)^\circ$, $\beta = 113.830(13)^\circ$, $\gamma = 90.352(12)^\circ$ and $V = 366.77(11)\ \text{\AA}^3$. It is isostructural with triclinic titanite and bond-topologically identical with titanite and other minerals of the titanite group. Żabińskiite crystallized along with (Al,Ta,Nb)-bearing titanites at increasing Ti and Nb, and decreasing Ta activities, almost coevally with polycrase-(Y) and euxenite-(Y) from Ca-contaminated fluxed melts or early hydrothermal fluids.

KEYWORDS: żabińskiite, titanite group, new mineral species, optical data, electron microprobe, crystal structure, NYF pegmatite, Piława Górna, Sudetes, Poland.

Introduction

THE titanite group, $(^7X)^{(6)Y}{}^{(4)}(\text{TO}_4)\text{O}$, currently comprises five mineral species: titanite, $(^7\text{Ca})^{(6)}\text{Ti}(\text{SiO}_4)\text{O}$ (grandfathered); malayaite, $(^7\text{Ca})^{(6)}\text{Sn}$

*E-mail: pieczka@agh.edu.pl

<https://doi.org/10.1180/minmag.2016.080.110>

(SiO_4)O (Alexander and Flinter, 1965; Higgins and Ribbe, 1977); vanadomalayaite, $(^{7}\text{Ca}^{(6)}\text{V}^{4+}(\text{SiO}_4)\text{O}$ (Basso *et al.*, 1994); natrotitanite, $(^{7}\text{Na}_{0.5}\text{Y}_{0.5})(^{6}\text{Ti}(\text{SiO}_4)\text{O}$ (Stepanov *et al.*, 2012); and žabińskiite, $(^{7}\text{Ca}^{(6)}(\text{Al}_{0.5}\text{Ta}_{0.5})(\text{SiO}_4)\text{O}$, which was approved recently by the Commission on New Minerals, Nomenclature and Classification of the International Mineralogical Association (IMA CNMNC) (Pieczka *et al.*, 2015b; IMA 2015-033). Titanite is a common accessory mineral in intermediate, felsic and alkaline plutonic rocks (diorites, granodiorites, granites, syenites, nepheline syenites, carbonatites, phoscorites, etc.) and their volcanic analogues, pegmatites, hydrothermal veins, alpine-type veins, gneisses, schists, skarns and marbles; malayaite is an early hydrothermal product, which may associate with a cassiterite–quartz assemblage, and a component of Sn-bearing skarns. Vanadomalayaite and natrotitanite are two extremely rare members of the group, each known from only one occurrence: in a manganese ore deposit exploited by the Valgraveglia (Gambatesa) Mine, Genova Province, Italy (Basso *et al.*, 1994) and the Verkhnee Espe rare-element deposit, Eastern Kazakhstan Province, Kazakhstan (Stepanov *et al.*, 2012), respectively.

Igneous titanite does not usually show extensive substitution and its composition is close to the end-member. As titanite crystallizes, it can incorporate various cations substituting for Ca^{2+} (Na^+ , Sr^{2+} , Mn^{2+} and $\text{Y}^{3+}+\text{Ln}^{3+}$) or Ti^{4+} (Al^{3+} , Fe^{3+} , Sb^{3+} , Sn^{4+} , Zr^{4+} , V^{4+} , Nb^{5+} and Ta^{5+}) (Sahama, 1946; Černý and Riva di Sanseverino, 1972; Clark, 1974; Higgins and Ribbe, 1976; Paul *et al.*, 1981; Hollabaugh and Foit, 1984; Sawka *et al.*, 1984; Groat *et al.*, 1985; Bernau and Franz, 1987; Woolley *et al.*, 1992; Basso *et al.*, 1994; Russell *et al.*, 1994; Černý *et al.*, 1995; Della Ventura *et al.*, 1999; Markl and Piazzolo, 1999; Tiepolo *et al.*, 2002; Chakhmouradian and Zaitsev, 2002; Chakhmouradian *et al.*, 2003; Chakhmouradian, 2004; Houzar *et al.*, 2008; Cempírek *et al.*, 2008; Lussier *et al.*, 2009; Stepanov *et al.*, 2012). Niobium and Ta are relatively common subordinate substituents at the Y site of the titanite structure. However, titanites with a substantial amount of these elements are uncommon. Generally, Nb-enriched titanites are associated with nepheline syenites and carbonatites (e.g. Woolley *et al.*, 1992; Chakhmouradian *et al.*, 2003; Chakhmouradian, 2004), whereas tantalum titanite, usually also enriched in Nb, is known from granitic pegmatites (e.g. Clark, 1974; Paul *et al.*, 1981; Groat *et al.*, 1985; Černý *et al.*, 1995; Uher *et al.*, 1998). The

presence of Nb^{5+} and Ta^{5+} , substituting for Ti^{4+} at the Y site, is either balanced by coupled 3-valent cations (Al^{3+} and Fe^{3+}), or is the result of an additional coupled replacement of Ca^{2+} by Na^+ at the X site, or Al^{3+} for Si^{4+} at the T site. To date, the most Ta- and Nb-enriched titanite is from Maršikov II pegmatite in northern Moravia, Czech Republic (Černý *et al.*, 1995). It contains up to 21.53 wt.% Ta_2O_5 (0.216 Ta atoms per formula unit, apfu) and up to 9.49 wt.% Nb_2O_5 (0.163 Nb apfu), with the highest Nb + Ta content (Nb < Ta) equal to 0.278 apfu in the Na-poor variety and 0.359 apfu in the Na-bearing variety. However, due to simultaneous substitutions at the X and Y sites and possible vacancy at the T site, none of these titanite varieties corresponds to a Ta-dominant species (Černý *et al.*, 1995). Liferovich and Mitchell (2006a) synthesized a high-(Al,Ta) analogue of titanite with composition $\text{Ca}(\text{Ti}_{0.4}\text{Al}_{0.3}\text{Ta}_{0.3})\text{SiO}_4\text{O}$ and concluded that solid solution involving the smaller cations might be stabilized at high pressure, suggesting the existence of a potentially new compound with ≥ 67 mol.% $\text{Ca}(\text{Al}_{0.5}\text{Ta}_{0.5})\text{SiO}_4\text{O}$ end-member. Other experimental data (*ibidem*) indicated that a titanite analogue with more than 50 mol.% of a $\text{NaTaSiO}_4\text{O}$ end-member is unlikely to exist.

In this paper, we describe žabińskiite (pronunciation: zhabijnskiit), a new mineral of the titanite group with dominance of $2^{\text{Y}}(\text{Ta} + \text{Nb})$ over $^{\text{Y}}\text{Ti}$ and $\text{Ta} \gg \text{Nb}$, as a result of the substitution $(\text{Ta,Nb})^{5+} + \text{Al}^{3+} \rightarrow 2^{\text{Y}}\text{Ti}^{4+}$, containing up to 24.85 wt.% Ta_2O_5 (0.260 Ta apfu) and up to 8.02 wt.% Nb_2O_5 (0.127 Nb apfu), and the highest Ta + Nb content of 0.344 apfu yet recorded. Žabińskiite was discovered in weakly fractionated parts of the Julianna system of anatectic pegmatites at Piława Górna, the Góry Sowie Block, Lower Silesia, SW Poland. Žabińskiite has been approved by the IMA CNMNC (proposal IMA 2015-033). The mineral is named to honour the late Professor Witold Žabiński (1929–2007) – one of the most eminent Polish mineralogists and one of the founders of the Mineralogical Society of Poland and its President in 1980–1994. The žabińskiite holotype (P37 specimen) is preserved at the Mineralogical Museum of the University of Wrocław, in the form of one polished, 1-inch in diameter, disc with the catalogue number MMWr IV7675. Žabińskiite is isostructural with triclinic titanite (Lussier *et al.*, 2009) and is bond-topologically identical with other members of the titanite group. Žabińskiite classifies in the class 9.AG.15 (Nesosilicates with additional anions; cations in $> [6] \pm [6]$ coordination)

in the classification of Strunz and Nickel (2001), whereas in the classification of Dana (Gaines *et al.*, 1997), it belongs to the class 52.04.03 Nesosilicate Insular SiO_4 Groups and O, OH, F and H_2O with cations in [6] and/or >[6] coordination/Titanite group, along with titanite (52.04.03.01), malayaite (52.04.03.02), vanadomalayaite (52.04.03.03) and natrotitanite (52.04.03.04).

Geological setting

Żabińskiite was found in a pegmatitic system exposed in an amphibolite-migmatite quarry of the Kompania Górnicza (formerly Dolnośląskie Surowce Skalne S.A Company) near the town of Piława Górna (50°42'11.77"N, 16°44'12.36"E), the Góry Sowie Block (GSB), ~50 km southwest of Wrocław, SW Poland. The GSB is one of the main tectono-stratigraphic units (~650 km²) of the Sudetes, the region that forms the NE margin of the Bohemian Massif and the NE termination of the European Variscides. The GSB consists mainly of gneisses and migmatites with minor amphibolites, and is considered to be a fragment of the lower crust (for details see Mazur *et al.*, 2006). The unit is a product of multistage evolution that culminated ~385–370 Ma in amphibolite-facies metamorphism and migmatization at temperatures of 775–910°C and pressures of 6.5–8.5 kbar, and was followed by rapid uplift and exhumation (Brueckner *et al.*, 1996; O'Brien *et al.*, 1997; Kryza and Fanning, 2007). Anatectic melts generated by partial melting of the metasedimentary–metavolcanic sequence were injected as pegmatites and granite-like bodies during decompression stages, forming small concordant segregations and N-trending discordant dykes in migmatized gneisses and amphibolites (Kryza, 1981; van Breemen *et al.*, 1988; Żelaźniewicz, 1990; Bröcker *et al.*, 1998; Timmermann *et al.*, 2000; Aftalion and Bowes, 2002; Gordon *et al.*, 2005). The Julianna pegmatitic system at Piława Górna, the largest pegmatitic occurrence in the GSB, displays a hybrid NYF (Nb–Y–F) + LCT (Li–Cs–Ta) signature (Szuszkiewicz *et al.*, 2013; Pieczka *et al.*, 2013; 2014; 2015a,c; 2016). The system consists of a series of coeval and co-genetic pegmatites ranging from homogeneous and relatively primitive dykes to simply zoned (border zone + wall zone + graphic intermediate zone + blocky feldspar intermediate zone + quartz core) weakly to moderately evolved NYF-affiliated bodies. The most common are moderately-evolved pegmatitic bodies with abundant rare-element-bearing mineralization, mainly (Fe,Mn)–(Ti,Sn)–(Nb,Ta)

and (REE,U)–(Nb,Ti,Ta) oxides [where REE = rare-earth elements], e.g. columbite-group minerals, ixiolites, ferrowodginite as well as samarskite-, euxenite-, fergusonite-group minerals, pyrochlore-supergrout minerals, zircon, monazite-(Ce), xenotime-(Y), allanite-(Ce) and -(Y), keiviite-(Y), pilawite-(Y) and uraninite (Pieczka *et al.*, 2013, 2014, 2015a). The most fractionated LCT-related parts of the Julianna system are represented by rare pods, up to a few metres in diameter, located in the central parts of swellings at intersections of larger pegmatitic dykes, where the quartz core would typically occur. They are formed of a centrally located spodumene–lepidolite core within a lithium-mica–cleavelandite–quartz unit, and accompanied by saccharoidal albite irregularly replacing the surrounding blocky feldspar and graphic units. The pods contain extremely fractionated Li- and Cs-bearing mineralization, including elbaite–liddicoatite–rossmanite tourmaline, pollucite, spodumene, Cs-bearing beryl and Li-micas (Pieczka *et al.*, 2016).

Small aggregates of (Al,Ta,Nb)-enriched titanite, together with epidote-group minerals and sometimes also with gadolinite-group minerals, occur in thin veinlets that fill fractures in blocky feldspars. Żabińskiite, ideally $\text{Ca}(\text{Al}_{0.5}\text{Ta}_{0.5})(\text{SiO}_4)\text{O}$, was found together with (Al,Ta,Nb)-bearing titanites, a bismuth-rich pyrochlore-group mineral and single plates of a K-mica in aggregates healing fractures in zircon intergrown with polycrase-(Y) and euxenite-(Y) in blocky feldspar.

Analytical methods

Optical properties of żabińskiite were obtained at the Department of Geological Sciences, University of Manitoba, Winnipeg, Canada, on a crystal extracted for structural studies. A spindle stage was used to orient the crystal for measurement of 2V by extinction curves (Bartelmehs *et al.*, 1992). The optical orientation (Table 1) was determined by transferring the crystal from the spindle stage to a single-crystal diffractometer and measuring the relative axial relations by X-ray diffraction.

Electron-microprobe analyses (70 spots) of żabińskiite and associated minerals were carried out at the Inter-Institute Analytical Complex for Minerals and Synthetic Substances of the University of Warsaw using a CAMECA SX 100 electron microprobe operating in wavelength-dispersive spectroscopy mode with an accelerating voltage of 20 kV, beam current of 15 nA, peak count-time of 20 s, background time of 10 s and a

beam diameter of 2 μm . Standards, analytical lines, diffracting crystals and mean detection limits (wt.%) were as follows: phlogopite – F ($K\alpha$, TAP, 0.15), albite – Na ($K\alpha$, TAP, 0.01), orthoclase – Al ($K\alpha$, TAP, 0.01), diopside – Si ($K\alpha$, TAP, 0.02), wollastonite – Ca ($K\alpha$, PET, 0.03), metallic Sc – Sc ($K\alpha$, PET, 0.02), rutile – Ti ($K\alpha$, PET, 0.03), V_2O_5 – V ($K\alpha$, LIF, 0.07), rhodonite – Mn ($K\alpha$, LIF, 0.06), hematite – Fe ($K\alpha$, LIF, 0.06), YAG – Y ($L\alpha$, TAP, 0.06), zircon – Zr ($L\alpha$, PET, 0.08), metallic Nb – Nb ($L\alpha$, PET, 0.10), cassiterite – Sn ($L\alpha$, PET, 0.07), metallic Ta – Ta ($M\alpha$, TAP, 0.07), vorlanite – U ($M\beta$, PET, 0.12). The raw data were reduced with the *PAP* routine of Pouchou and Pichoir (1985). The empirical formulae of žabińskiite and associated titanite were calculated on the basis of 3 cations per formula unit, with H_2O in the form of OH^- groups calculated on the basis of stoichiometry to 5 (O,F,OH) anions, and assuming $\text{Fe}_{\text{total}} = \text{Fe}^{3+}$. Representative compositions of various members of the titanite group from the Piława Górna pegmatites are presented in Table 2. Table 3 gives the statistics of analytical results for the most Ta-enriched crystal of žabińskiite.

Raman spectroscopic and electron-backscatter diffraction (EBSD) studies were done at the Division of Geological and Planetary Sciences, California Institute of Technology, California, USA. Raman spectra were obtained using a Renishaw M-1000 microRaman spectrometer with two laser wavelengths (514.4 and 783.5 nm) that result in ~ 5 mW on the sample. Ten 20-second scans were averaged on spots of ~ 1.5 μm in diameter through a $100\times$ objective with polarization removed by a dual silica-wedge depolarizer. No indication of sample damage was noted. All the traces were corrected for instrumental artifacts, and had cosmic-ray spikes removed. They were then manually corrected for the apparent baseline by visual inspection and subtraction.

Single-crystal EBSD analyses at a sub-micrometre scale were done using the method of Ma and Rossman (2008, 2009) with an HKL EBSD system on a ZEISS 1550VP scanning electron microscope, operating at 20 kV and 6 nA in focused-beam mode, with a 70° tilted stage and in a variable-pressure mode (25 Pa). The structure was determined by matching the experimental EBSD pattern with the Al-bearing titanite structure.

Single-crystal X-ray diffraction measurements were undertaken at the Department of Geological Sciences, University of Manitoba, Winnipeg, Canada, on a crystal $5\text{ }\mu\text{m} \times 7\text{ }\mu\text{m} \times 20\text{ }\mu\text{m}$ attached to a tapered glass fibre and mounted on a Bruker D8

three-circle diffractometer equipped with a rotating-anode generator (Mo $K\alpha$ X-radiation), multilayer optics and an APEX-II detector. A total of 7073 intensities was collected to $60^\circ 2\theta$ using 50 s per 0.3° frame-width with a crystal-to-detector distance of 5 cm. Empirical absorption corrections (*SADABS*; Sheldrick, 2008) were applied and equivalent reflections were merged, resulting in 1068 unique reflections. Unit-cell dimensions were obtained by least-squares refinement of the positions of 3945 reflections with $I > 10\sigma I$ and are given in Table 4, together with other information pertaining to data collection and structure refinement. The structure was refined to an *R*1 index of 2.37%. Atom positions and equivalent isotropic-displacement parameters are given in Table 5, selected interatomic distances in Table 6, and refined site-scattering values (Hawthorne *et al.*, 1995) and assigned site-populations in Table 7. A powder X-ray diffraction pattern was not measured because of the compositional heterogeneity of the material. However, in Table 8 we provide a two-dimensional pattern by collapsing the three dimensional diffraction data into two dimensions, using an option in *XPREP* (Sheldrick, 2000); this means we can guarantee that the pattern is representative of the chemical composition and crystal structure provided here.

Physical and optical properties

Žabińskiite occurs together with (Al,Ta,Nb)- and (Al,F)-bearing titanites in compositionally inhomogeneous aggregates present as fracture fillings in a fractured crystal of zircon intergrown with euxenite-(Y) and polycrase-(Y) (Fig. 1). The žabińskiite–titanite aggregates reach $\sim 120\text{ }\mu\text{m} \times 70\text{ }\mu\text{m}$ in size, while individual grains of minerals forming these aggregates do not exceed 25 μm long. The aggregates commonly show irregular patchy and mosaic zoning and exsolution-like domains, less frequent oscillatory zoning.

Žabińskiite is transparent, brownish, with a white streak and vitreous lustre. It is non-fluorescent. Neither cleavage nor parting is observed and the fracture is uneven. The mineral is brittle, having a Mohs hardness of ~ 5 . Density was not measured due to small dimensions and compositional heterogeneity of the crystals. The density calculated on the basis of molar weight and unit-cell volume for the refined crystal of titanian žabińskiite with the composition $\text{Ca}(\text{Ti}_{0.46}\text{Al}_{0.27}\text{Ta}_{0.15}\text{Nb}_{0.09}\text{Fe}_{0.02}^{3+})_{\Sigma=1}\text{SiO}_4(\text{O}_{0.95}\text{F}_{0.05})$ is equal to 3.897 g cm^{-3} . However, due to varying, though always significant

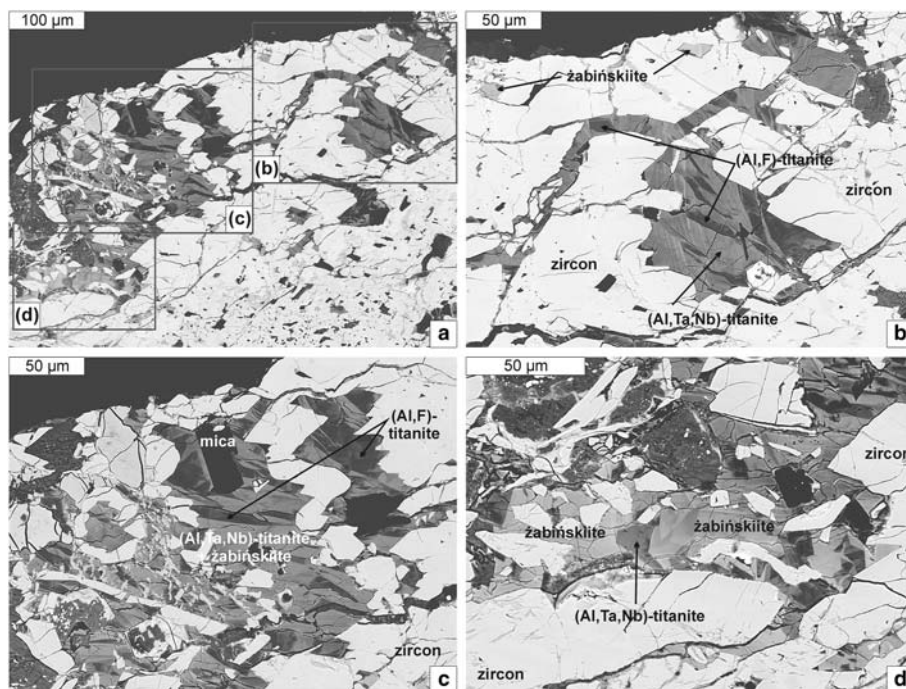


FIG. 1. A fragment of a fractured zircon crystal with zoned inclusions of (Al,Ta,Nb)-bearing titanite with $Ta + Nb + Al < Ti$ and žabińskiite with $Ta + Nb + Al > Ti$. Enlarged regions with žabińskiite grains are marked as (b), (c) and (d) in image (a). Note the common fine-scale irregular mosaic zoning (c, d), less frequent oscillatory zoning (b, d) in žabińskiite and (Al,Ta,Nb)-bearing titanite, as well as irregular patchy exsolutions of (Al,F)-bearing titanite (b, c) within these two minerals.

TABLE 1. Optical orientation of žabińskiite

	a	b	c
X	12.5°	83.2°	103.4°
Y	100.1°	20.0°	69.8°
Z	97.4°	108.7°	24.6°

Ta contents in different žabińskiite crystals, the calculated density depends strongly on composition. For example, for žabińskiite with the highest measured content of Ta + Nb, the density should increase to $\sim 4.1 \text{ g cm}^{-3}$, and for the end-member composition, it should be $\sim 4.5 \text{ g cm}^{-3}$.

Žabińskiite is non-pleochroic (uniformly yellowish brown in all optical directions), biaxial (–), with mean refractive indices ≥ 1.89 (589 nm) (refractive indices were not measured as the required liquids are forbidden by Polish and Canadian health and safety regulations) and $2V_{\text{meas.}} = 96.9(5)^\circ$.

Dispersion was not measured and colour evaluation was difficult due to very small dimensions of the extracted crystal and the ‘edge effects’ observed in immersion. The optical orientation is presented in Table 1.

Chemical composition

Tiny grains of (Al,Ta,Nb)-bearing titanite-group minerals from Piława Górna show strong compositional heterogeneity, similar to other Nb- and Ta-enriched titanites reported in the literature (e.g. Clark, 1974; Černý *et al.*, 1995; Chakhmouradian, 2004; Houzar *et al.*, 2008). In Fig. 1, žabińskiite and (Al,Ta,Nb)-bearing titanite are represented by light- to medium-grey crystals showing common irregular patchy and mosaic zoning and less frequent oscillatory zoning in the back-scattered electron (BSE) images, while (Al,F)-bearing and Nb- and Ta-poor titanite occurs as dark grey exsolution-like domains (Table 2 and 3). In the diagram $Y^{3+} (= Al + Fe) - Y^{4+} (= Ti + Sn + V + Zr) -$

TABLE 2. Representative compositions of the Piława Górna titanite-group minerals (wt.%)

No. analyses	Al-rich titanite		(Al,Ta,Nb)-rich titanite		Żabińskiite		Nb analogue of żabińskiite (?)	
	2	24	55	46	35	37	13	31
Nb ₂ O ₅	0.32	3.01	5.85	4.61	4.80	6.15	7.58	7.14
Ta ₂ O ₅	0.69	5.11	10.15	15.38	24.85	21.47	11.98	11.61
SiO ₂	31.07	29.78	28.21	27.21	25.71	25.83	27.93	27.99
TiO ₂	24.77	20.37	20.71	18.24	10.15	10.64	15.66	14.02
VO ₂	0.09	0.15	0.09	0.06	0.00	0.00	0.09	0.07
ZrO ₂	b.d.l.	0.08	0.06	0.14	0.11	0.28	0.15	0.06
SnO ₂	0.07	0.36	1.49	0.52	0.40	1.29	0.93	0.41
Al ₂ O ₃	10.82	9.97	5.62	5.99	7.45	6.81	7.71	9.28
Fe ₂ O ₃	0.07	0.41	0.38	0.35	0.99	1.23	0.53	0.57
CaO	28.95	27.87	26.36	25.63	23.82	24.25	26.25	26.51
Na ₂ O	0.02	b.d.l.	0.03	0.04	0.21	0.10	0.02	0.05
H ₂ O _(calc.)	0.46	0.52	0.07	0.09	0.04	0.05	0.22	0.33
F	2.81	1.74	0.30	0.22	0.21	0.12	0.42	1.00
–O = F2	–1.18	–0.73	–0.13	–0.09	–0.09	–0.05	–0.18	–0.42
Total	98.95	98.63	99.21	98.40	98.66	98.17	99.30	98.61
Atoms per formula unit								
<i>X</i> site								
Ca ²⁺	0.990	0.995	0.995	1.000	0.982	0.996	0.998	1.002
Na ⁺	0.001	0.000	0.002	0.003	0.016	0.008	0.002	0.003
<i>Y</i> site								
Nb ⁵⁺	0.005	0.045	0.093	0.076	0.084	0.107	0.122	0.114
Ta ⁵⁺	0.006	0.046	0.097	0.152	0.260	0.224	0.116	0.111
Ti ⁴⁺	0.595	0.510	0.549	0.500	0.294	0.307	0.418	0.372
V ⁴⁺	0.002	0.004	0.002	0.002	0.000	0.000	0.002	0.002
Zr ⁴⁺	0.000	0.001	0.001	0.002	0.002	0.005	0.003	0.001
Sn ⁴⁺	0.001	0.005	0.021	0.008	0.006	0.020	0.013	0.006
Al ³⁺	0.399	0.383	0.229	0.248	0.328	0.298	0.313	0.374
Fe ³⁺	0.002	0.010	0.010	0.009	0.029	0.036	0.014	0.015
<i>T</i> site								
Si ⁴⁺	0.992	0.992	0.995	0.991	0.990	0.990	0.991	0.988
Al ³⁺	0.008	0.008	0.005	0.009	0.010	0.010	0.009	0.012
O ^{2–}	4.619	4.700	4.949	4.952	4.965	4.972	4.900	4.811
OH [–]	0.098	0.116	0.018	0.022	0.009	0.013	0.052	0.078
F [–]	0.283	0.184	0.033	0.026	0.026	0.015	0.048	0.111
Compound	mol%							
Ca(Ti,Sn,Zr,V)SiO ₄ O	59.3	51.7	57.1	51.3	30.1	33.3	43.6	38.3
Ca[Al _{0.5} (Ta,Nb) _{0.5}]SiO ₄ O	0.4	16.5	36.5	43.3	63.5	62.9	47.2	42.2
Na(Ta,Nb)SiO ₄ O	0.1	0.0	0.2	0.3	1.6	0.8	0.2	0.3
Ca(Ta,Nb)AlO ₄ O	0.8	0.8	0.5	0.9	1.0	1.0	0.9	1.2
CaAlSiO ₄ (F,OH)	39.5	30.9	5.6	4.1	3.9	1.9	10.0	17.9
Ta/(Ta + Nb)	0.562	0.505	0.510	0.667	0.757	0.677	0.487	0.494

Notes: Mn, Sc, Y and U were below the detection limit.

Y^{5+} (=Nb + Ta), most compositions of titanite-group minerals lie along the line Ca(Ti,Sn,V,Zr)(SiO₄)O – Ca[Al_{0.5}(Ta,Nb)_{0.5}](SiO₄)O, suggesting

simple solid-solution between the Y^{4+} -dominant end-member CaTi(SiO₄)O (Ti >> Sn, V and Zr), and the end-members Ca[Al_{0.5}Ta_{0.5}](SiO₄)O and

TABLE 3. Average composition of žabińskiite.

Constituent	wt.% ($n = 10$) ⁽¹⁾	Range	SD		apfu ⁽²⁾	SD (apfu)
Nb ₂ O ₅	4.68	4.10–5.32	0.33	Nb ⁵⁺	0.081	0.006
Ta ₂ O ₅	24.20	23.42–24.85	0.51	Ta ⁵⁺	0.251	0.006
SiO ₂	25.88	25.65–26.42	0.23	Si ⁴⁺	0.988	0.005
TiO ₂	10.37	9.77–10.85	0.36	Ti ⁴⁺	0.298	0.010
VO ₂	0.04	0.00–0.16	0.06	V ⁴⁺	0.001	0.002
ZrO ₂	0.05	0.00–0.11	0.05	Zr ⁴⁺	0.001	0.001
SnO ₂	0.35	0.13–0.54	0.11	Sn ⁴⁺	0.005	0.002
Al ₂ O ₃	7.82	7.42–8.45	0.38	Al ³⁺	0.352	0.016
Fe ₂ O ₃	0.99	0.63–1.62	0.36	Fe ³⁺	0.029	0.010
CaO	23.97	23.63–24.24	0.20	Ca ²⁺	0.980	0.007
Na ₂ O	0.20	0.16–0.24	0.03	Na ⁺	0.015	0.002
F ₂	0.39	0.21–0.65	0.13	F [−]	0.047	0.015
H ₂ O ⁽³⁾	0.03	0.00–0.17	0.05	OH [−]	0.007	0.010
−O = F ₂	−0.16	−0.27 – −0.09	0.05	O ^{2−}	4.946	
Total	98.80	98.10–99.46	0.50			

Notes: Mn, Y and U were below the detection limit.

(1) Average composition of 10 analyses of crystals richest in (Ta, Nb) is presented in Fig. 1d; (2) Normalized on the basis of X + Y + T = 3 apfu; (3) calculated from stoichiometry; SD – standard deviation.

Ca(Al_{0.5}Nb_{0.5})(SiO₄)O (Ta > Nb) (Fig. 2). Some of the compositions show Ti + Sn + V + Zr > Al + Fe³⁺ + Nb + Ta (medium grey zones in the aggregates in Fig. 1), and represent (Al,Ta,Nb)-bearing titanite. However, many analyses of the lightest domains give Ti + Sn + V + Zr < Al + Fe³⁺ + Nb + Ta, Ta > Nb. These compositions cross beyond the border of 50 mol.% Ca[Al_{0.5}(Ta,Nb)_{0.5}](SiO₄)O and, due to coupled heterovalent substitutions at a single structural site, i.e. valency-imposed double site-occupancy as explained by Hatert and Burke (2008), represent žabińskiite, a new aluminioantitalian mineral in the titanite group. The analyses have the highest Ta content reported in a titanite-group mineral, attaining 24.85 wt.% Ta₂O₅ (0.260 Ta apfu) at the Nb + Ta sum equal to 0.344 apfu (Table 2). Low amounts of Na (≤0.24 wt.% Na₂O, 0.018 apfu Na) and minor Si deficiency (~0.008 apfu) indicate a negligible role of the two coupled substitutions: Na⁺ + (Ta,Nb)⁵⁺ → ^XCa²⁺ + ^YTi⁴⁺ and (Ta,Nb)⁵⁺ + Al³⁺ → ^YTi⁴⁺ + Si⁴⁺ and, consequently, low mole fractions of end-members Na(Ta,Nb)(SiO₄)O and Ca(Ta,Nb)(AlO₄)O. On the other hand, a strong positive correlation ($r^2 = 0.836$) between 5-valent and 3-valent Y cations, (Ta,Nb)⁵⁺ = 0.975 · (Al,Fe)³⁺ − 0.039 (Fig. 3a), indicates that the coupled substitution (Al,Fe)³⁺ + (Ta,Nb)⁵⁺ → 2^YTi⁴⁺ is mostly responsible for the large amounts of Al³⁺, Ta⁵⁺ and Nb⁵⁺ (Ta > Nb) at the Y site and the

formation of žabińskiite, Ca(Al_{0.5}Ta_{0.5})(SiO₄)O. This substitution was regarded as crucial for the incorporation of 5-valent cations into the structure of (Al,Ta,Nb)-bearing titanite by Paul *et al.* (1981), Groat *et al.* (1985), Russell *et al.* (1994), Černý *et al.* (1995), Houzar *et al.* (2008) and Cempírek *et al.* (2008). A small excess of ^YAl over (Ta + Nb) in žabińskiite and (Al,Ta,Nb)-bearing titanite, and the relatively steep linear relation of F vs. excess ^YAl, $F = 0.697 \cdot (Al + Fe^{3+} + Na - Nb - Ta) - 0.002$, $r^2 = 0.48$ (Fig. 3b), point to the subordinate substitution (Al,Fe)³⁺ + (F,OH)[−] → ^YTi⁴⁺ + O^{2−} with $F \gg OH$, responsible for the presence of some CaAl(SiO₄)(F,OH) component. This component becomes more important in domains of Ta- and Nb-poor (Al,F)-bearing titanite. Such titanite also has low Na contents (≤0.02 wt.% Na₂O) and shows a steeper linear trend between F and excess ^YAl, $F = 0.867 \cdot (Al + Fe^{3+} + Na - Nb - Ta) - 0.062$, $r^2 = 0.82$ (Fig. 3b), suggesting a stronger enrichment in F due to higher ^YAl content, as well as higher amounts of OH compared to (Al,Ta,Nb)-bearing titanite and žabińskiite. Consequently, Ta- and Nb-poor compositions represent a simple solid solution between the ^YAl⁴⁺-dominant end-member CaTi(SiO₄)O and the ^YAl-dominant end-members, CaAl(SiO₄)F and CaAl(SiO₄)OH.

In the diagram ^YAl+Na-Nb-Ta – Ti+Sn+V+Zr – 2(Nb+Ta-Na-^YAl) (Fig. 4), which discriminates

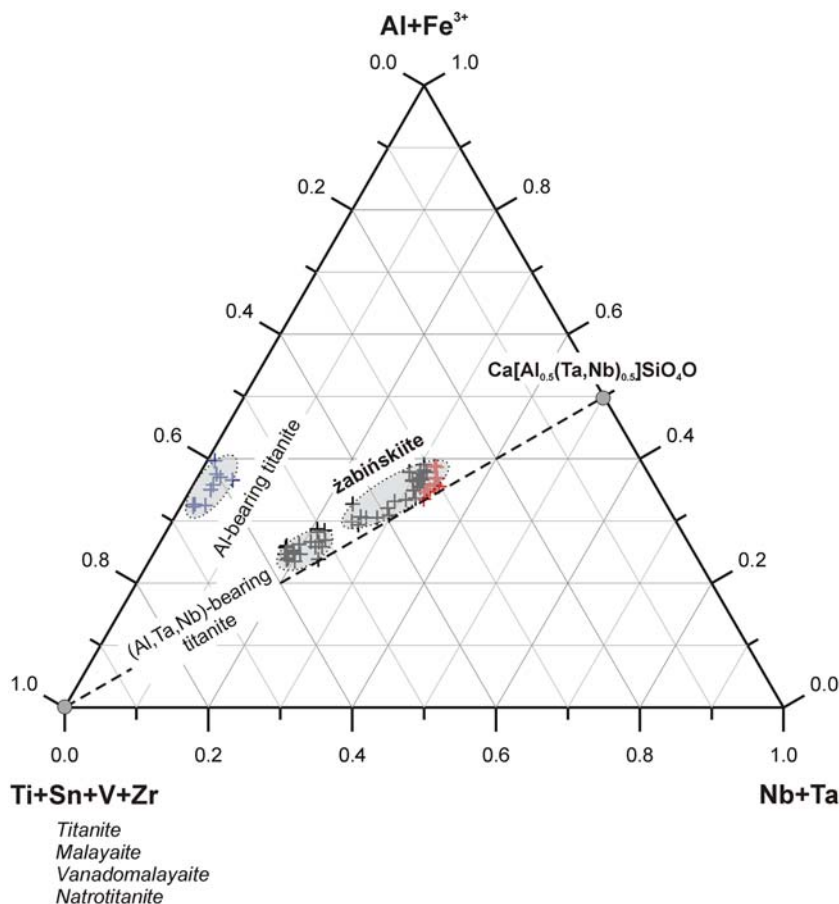


FIG. 2. Compositions of titanite-group minerals from the žabińskiite-bearing pegmatite from Piława Górna plotted in the ternary system $Y(\text{Al} + \text{Fe})^{3+} - Y(\text{Ti} + \text{Sn} + \text{V} + \text{Zr})^{4+} - Y(\text{Nb} + \text{Ta})^{5+}$. Symbols: red crosses – analyses with the highest Ta contents, used in the formula calculation (Table 2); black crosses – the remaining analyses of the titanite–žabińskiite solid solution; dark blue crosses – analyses of the (Al,F)-bearing titanite.

between žabińskiite, titanite/malayaite/vanadomalayaite/natrotitanite, and F- and OH-bearing $Y\text{Al}$ analogues of titanite, all (Al,Ta,Nb)-bearing compositions plot along the titanite–žabińskiite side of the triangle, straddling the border between the fields of Y^{4+} -dominant titanite-group varieties (titanite, malayaite, vanadomalayaite and natrotitanite) and a new group of $(Y^{3+} + Y^{5+})$ -dominant varieties with žabińskiite, $\text{Ca}[\text{Al}_{x/2}(\text{Ta},\text{Nb})_{x/2}\text{Ti}_{1-x}]\text{SiO}_4\text{O}$, where $x > 0.5$, as a Ta-dominant natural representative. The diagram corroborates continuous solid-solution between the end-members in the range 58–30 mol.% titanite + malayaite + vanadomalayaite ($\text{Ti} \gg \text{Sn} \approx \text{V}$; end-member natrotitanite is absent), 35–65 mol.% žabińskiite + its Nb analogue, and 0–9 mol.% of

Al- and (F,OH)-bearing titanite. On the other hand, Al-bearing, Nb- and Ta-poor titanite represents a solid solution of 58–67 mol.% titanite + malayaite + vanadomalayaite, 2–10 mol.% žabińskiite + its Nb analogue and 29–39 mol.% Al- and (F,OH)-bearing titanite. The average composition of (Al,Ta,Nb)-richest žabińskiite grains, forming the aggregate on the left side of Fig. 1d, corresponds to the formula $(\text{Ca}_{0.980}\text{Na}_{0.015})_{\Sigma=0.995}(\text{Al}_{0.340}\text{Fe}_{0.029}\text{Ti}_{0.298}\text{V}_{0.001}\text{Zr}_{0.001}\text{Sn}_{0.005}\text{Ta}_{0.251}\text{Nb}_{0.081})_{\Sigma=1.005}[(\text{Si}_{0.988}\text{Al}_{0.012})\text{O}_{4.946}\text{F}_{0.047}(\text{OH})_{0.007}]_{\Sigma=5.000}$. This average composition may be interpreted as a member of a complex five-component solid-solution series having 60.7 mol.% $\text{Ca}[\text{Al}_{0.5}(\text{Ta},\text{Nb})_{0.5}](\text{SiO}_4)\text{O}$, 30.3 mol.% titanite with negligible Sn, Zr and V, 6.4 mol.% $\text{CaAl}(\text{SiO}_4)(\text{F,OH}) (\text{Fe}^{3+})$.

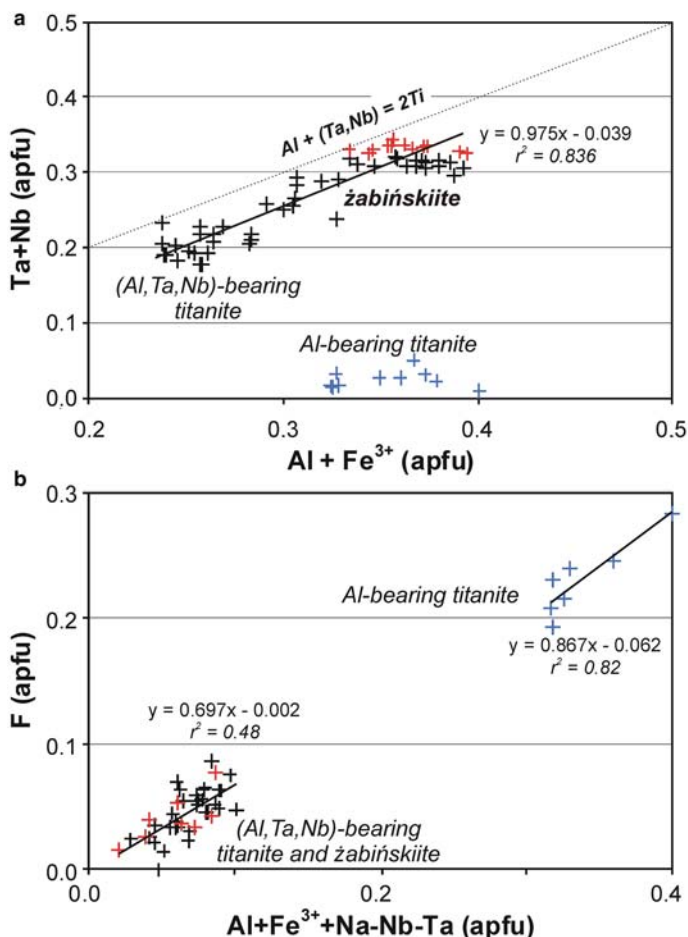


FIG. 3. Variation of: (a) 5-valent vs. 3-valent Y-site cations in titanite-group minerals from the žabińskiite-bearing pegmatite from Piława Górna. All compositions show a surplus of $Al + Fe^{3+}$ over $Ta + Nb$. The dotted line shows the substitution $Al + (Ta,Nb) \rightarrow 2^{Y}Ti$; (b) F vs. excess $^{Y}(Al + Fe^{3+})$ over $Ta + Nb$. In both plots, solid lines show the linear regression. The amounts of $Al + Fe^{3+}$ introduced by the substitutions $(Ta,Nb) + Al \rightarrow ^{Y}Ti + ^{7}Si$ and $0.5(Ta,Nb) + 0.5Al \rightarrow ^{Y}Ti$ have been deducted from the total amount of $Al + Fe^{3+}$ prior to plotting. Symbols as in Fig. 2.

added to ^{Y}Al), 1.5 mol.% $Na(Ta,Nb)SiO_4O$ and 1.2 mol.% $Ca(Ta,Nb)AlO_4O$. This composition of žabińskiite conforms with compositional data for synthetic (Al,Ta)-bearing titanites (Liferovich and Mitchell, 2006a,b). Liferovich and Mitchell (2006a, p. 73) concluded that “at ambient conditions, titanite can contain up to 20 mol.% $NaTaSiO_4O$ or 60 mol.% $Ca(Al_{0.5}Ta_{0.5})(SiO_4)O$ ”, and “these limits might differ in natural samples due to combinations with substitutions involving fluorine and/or hydroxyl replacing oxygen together with vacancies at cationic sites”. Furthermore

(*ibidem*, p.82), they find that “the solid solution involving the smaller cations, theoretically might be stabilized at high pressure suggesting the existence of a potentially new compound with ≥ 67 mol.% $Ca(Al_{0.5}Ta_{0.5})(SiO_4)O$ end-member”. In the Piława Górna material, the highest content of $Ca[Al_{0.5}(Ta,Nb)_{0.5}](SiO_4)O$ compound reaches 63.5 mol.% (Table 2) and most of the analyses with the highest Ta and Nb enrichment also show a noticeable increase of Al at almost constant $Ta + Nb$ contents (Fig. 3a). Due to the limited replacement of $^{Y}Ti^{4+}$ by the quasi-tetravalent aggregate cation

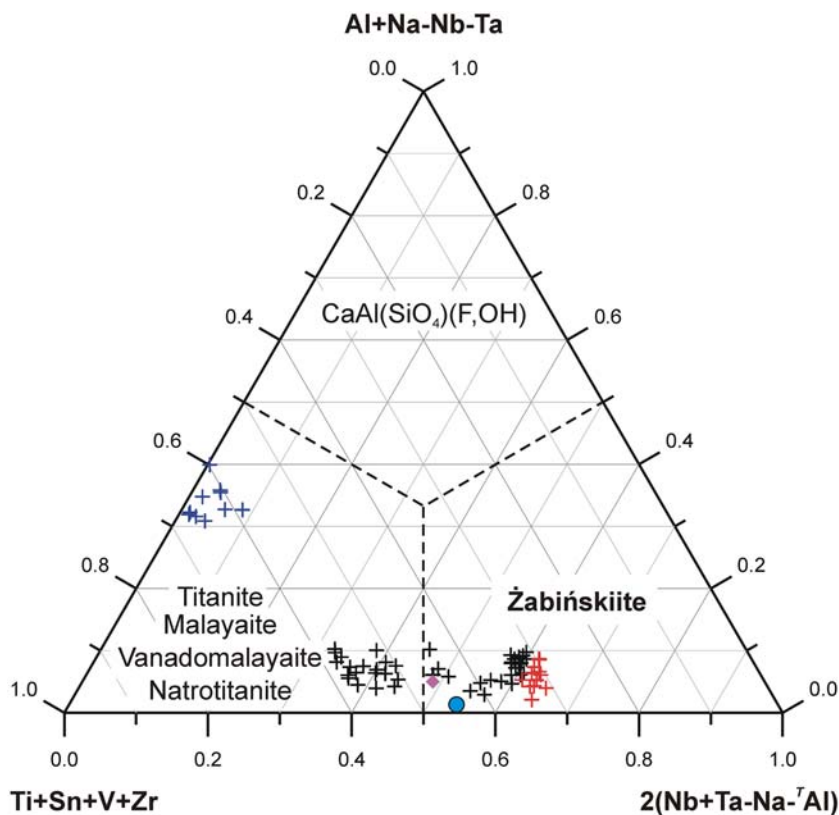


FIG. 4. Compositions of titanite-group minerals from the žabiňskiite-bearing pegmatite from Piława Górna classified on the basis of the substitutions $0.5\text{Al} + 0.5(\text{Ta,Nb}) \rightarrow {}^{\text{Y}}\text{Ti}$ and $(\text{Al,Fe})^{3+} + (\text{F,OH})^{-} \rightarrow {}^{\text{Y}}\text{Ti} + \text{O}$ in the diagram (titanite/malayaite/vanadomalayaite/natrotitanite) – žabiňskiite – (a hypothetical $\text{CaAl}(\text{SiO}_4)(\text{F,OH})$ titanite-like phase). The amounts of $\text{Al} + \text{Fe}^{3+}$ and $\text{Nb} + \text{Ta}$ introduced by the substitutions $\text{Na} + (\text{Ta,Nb}) \rightarrow {}^{\text{X}}\text{Ca} + {}^{\text{Y}}\text{Ti}$ and $(\text{Ta,Nb}) + \text{Al} \rightarrow {}^{\text{Y}}\text{Ti} + {}^{\text{Z}}\text{Si}$ have been deducted from the total amount of $\text{Al} + \text{Fe}^{3+}$ and $\text{Nb} + \text{Ta}$ prior to plotting. Symbols: violet diamond – a crystal of titanian žabiňskiite with refined structure; blue circle – (Al,Ta,Nb) -bearing titanite (žabiňskiite) from the Maršikov pegmatite (analysis 33cl; Černý *et al.*, 1995), the remaining symbols as in Fig. 2.

$[\text{Al}_{0.5}(\text{Ta,Nb})_{0.5}]^{4+}$, žabiňskiite compositions correspond to the simplified formula $\text{Ca}[\text{Al}_{x/2}(\text{Ta,Nb})_{x/2}\text{Ti}_{1-x}](\text{SiO}_4)\text{O}$, where $x > 0.5$.

Raman spectroscopy

Raman spectra were obtained at four spots, all corresponding to žabiňskiite, although with different compositions. The compositions at spots 1–3 vs. spot 4 are richer in $\text{Ca}[\text{Al}_{0.5}(\text{Ta,Nb})_{0.5}](\text{SiO}_4)\text{O}$ compound (the respective molar contents in %: 57.9, 63.5 and 56.8 vs. 42.2), and are accompanied by increasing titanite (32.0; 30.1; 32.3 vs. 38.3) and $\text{CaAl}(\text{SiO}_4)(\text{F,OH})$ (7.7; 3.9; 8.5 vs. 18.0), and completed by $\text{Na}(\text{Ta,Nb})(\text{SiO}_4)\text{O}$ (1.2; 1.6; 1.3;

0.3) and $\text{Ca}(\text{Ta,Nb})(\text{AlO}_4)\text{O}$ (1.2; 1.0; 1.1; 1.2). All spectra show strong consistency between the green and red laser excitations (Fig. 5a), which means that they do not originate from fluorescence; however, the band near 1400 cm^{-1} , obtained with the 783.5 nm laser, may result from fluorescence. The exact band heights are somewhat subjective because of the arbitrary baseline correction. In many of the spectra, the baseline background was more intense than any of the Raman or fluorescence bands. Wavenumbers obtained with the 514.5 nm laser for the spot 2 spectrum, recorded in a zone of the Ta- and Nb-richest žabiňskiite with the composition listed in Table 2, are: 341, 431, 487, 581, 642, 835 and 997 cm^{-1} . Comparison of the žabiňskiite spectrum with that of a standard titanite

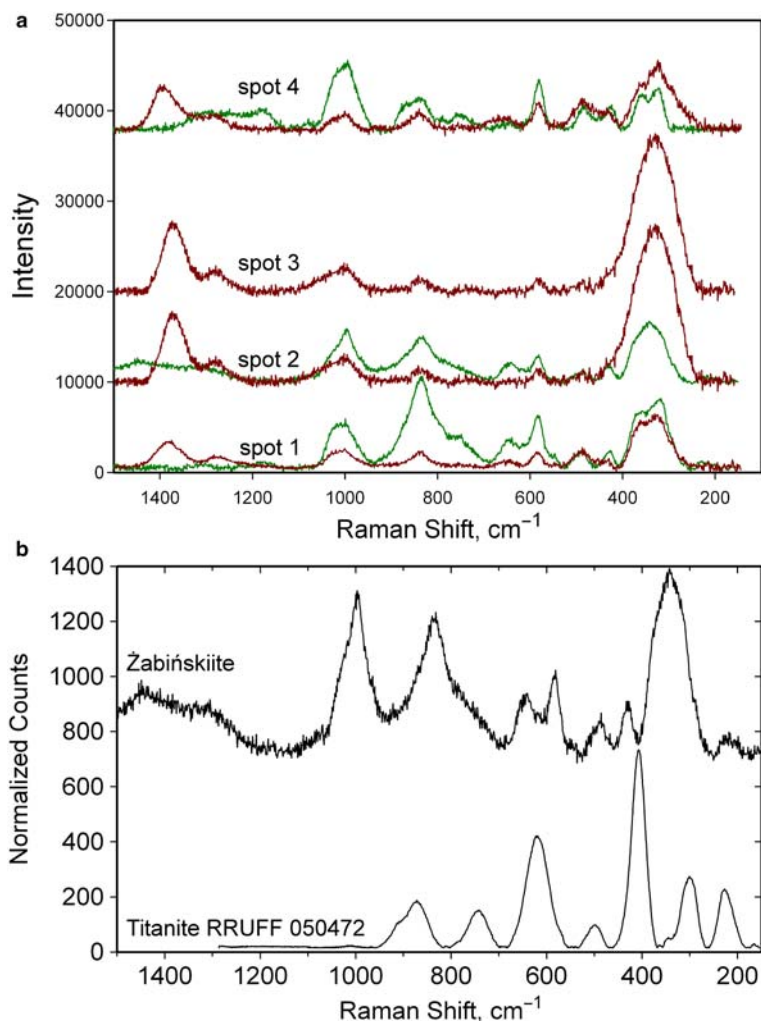


FIG. 5. (a) Raman spectra of žabińskiite in green (514.4 nm laser; green trace) and red (783.5 nm, brown trace) laser illumination; (b) comparison of the Raman spectrum of žabińskiite to a standard titanite spectrum from the RRUFF database (<http://rruff.info/Titanite/R050472>).

spectrum from the RRUFF database (<http://rruff.info/>) (Fig. 5b) shows that although the number of bands is similar in each spectrum, the positions of the bands differ, reflecting some differences between the structures of triclinic žabińskiite and monoclinic titanite.

Hollabaugh and Foit (1984), with mean angular deviations of $< 1^\circ$. No errors are stated for the presented data because the cell parameters are taken directly from the data of the matching phase of Hollabaugh and Foit (1984).

Electron-back-scattered diffraction (EBSD)

Single-crystal EBSD patterns (Fig. 6) were indexed with the titanite structure ($A2/a$) to give a best fit based on unit-cell data for the titanite of

Crystal structure

At room temperature, titanite close to end-member composition has a monoclinic structure with $P2_1/a$ symmetry (Higgins and Ribbe, 1976; Speer and

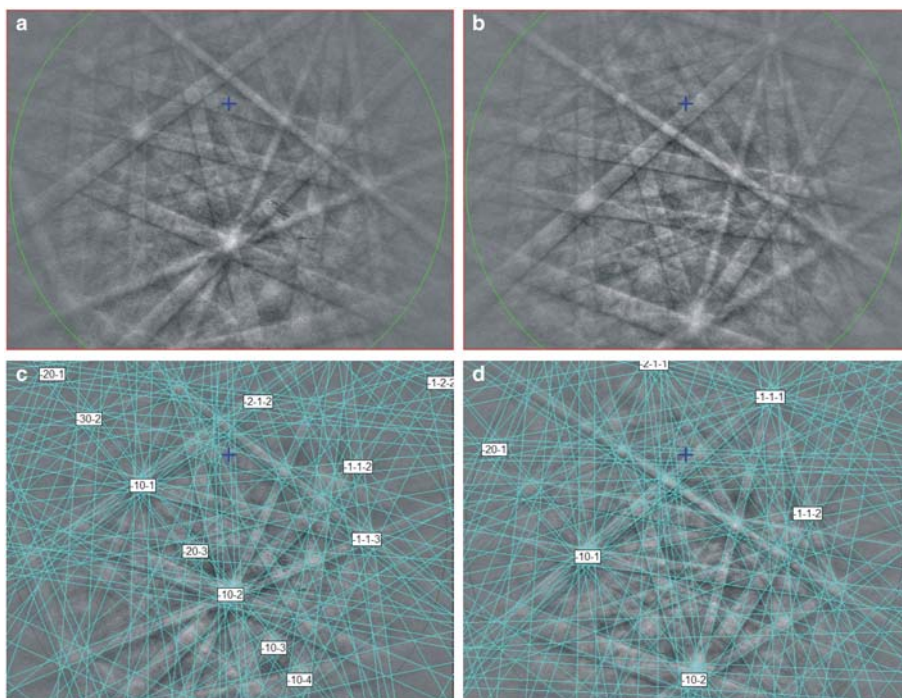


FIG. 6. EBSD patterns of žabiňskiite (a, b); the patterns indexed with the $A2/a$ titanite cell (Hollabaugh and Foit, 1984) (c, d).

Gibbs, 1976; Taylor and Brown, 1976; Bismayer *et al.*, 1992; Zhang *et al.*, 1995; Meyer *et al.*, 1996; Kek *et al.*, 1997; Beirau *et al.*, 2014). At higher temperature and/or pressure, and in structures with significant substitutions at the Y or $X+Y$ sites, a

phase transition results in transformation to the space-group $A2/a$. Transformation to a triclinic structure with space group $A\bar{1}$ was noted by Rath *et al.* (2003) in malayaite, $(\text{CaSnSiO}_4\text{O})$ at $P=4.95(1)$ GPa, and Ellemann-Olsen and Malcherek

TABLE 4. Miscellaneous information for žabiňskiite.

a (Å)	7.031(2)	Crystal size (μm)	$5 \times 7 \times 20$
b	8.692(2)	Radiation	MoK α
c	6.561(2)	No. of reflections	7073
α (°)	89.712 (11)°	No. unique reflections	1068
β	113.830 (13)	No. with ($F_o > 4\sigma F$)	1056
γ	90.352 (12)°		
V (Å ³)	366.77 (18)	R_{int} %	0.93
Space group	$A\bar{1}$	R_1 %	2.37
Z	4	wR_2 %	5.71
		No. of parameters	79

Cell content: 4 $\text{Ca}[\text{Al}_{0.27}\text{Fe}_{0.02}(\text{Ta},\text{Nb})_{0.25}\text{Ti}_{0.46}](\text{SiO}_4)\text{O}$

$R_1 = \Sigma(|F_o| - |F_c|)/\Sigma|F_o|$

$wR_2 = [\Sigma w(F_o^2 - F_c^2)^2 / \Sigma w(F_o^2)^2]^{1/2}$, $w = 1/[\sigma^2(F_o^2) + (0.0160 P)^2 + 4.09 P]$ where

$P = (\text{Max}(F_o^2, 0) + 2F_c^2)/3$

TABLE 5. Site coordinates and equivalent-displacement parameters (\AA^2) for żabińskiite.

Atom	<i>x</i>	<i>y</i>	<i>z</i>	<i>U</i> _{eq}
<i>Ca</i>	0.23749(15)	0.66914(9)	0.49706(13)	0.0281(2)
<i>M</i> (1)	0	½	0	0.0116(3)
<i>M</i> (2)	½	½	0	0.01122(12)
<i>Si</i>	0.75377(14)	0.68338(10)	0.50325(15)	0.0119(2)
O(1)	0.7525(4)	0.5690(3)	−0.0019(4)	0.0151(5)
O(2)	0.9146(4)	0.5676(3)	0.6898(4)	0.0180(5)
O(3)	0.3841(4)	0.7110(3)	0.8992(4)	0.0154(5)
O(4)	−0.4058(4)	0.5651(3)	0.3159(4)	0.0174(5)
O(5)	0.1171(4)	0.7071(3)	−0.8977(4)	0.0153(5)

TABLE 6. Selected interatomic distances (\AA) for żabińskiite.

<i>Ca</i> –O(1)	2.277(3)	<i>Si</i> –O(2)	1.635(3)
<i>Ca</i> –O(2)	2.412(3)	<i>Si</i> –O(3)	1.646(3)
<i>Ca</i> –O(3)	2.442(3)	<i>Si</i> –O(4)	1.647(3)
<i>Ca</i> –O(3)	2.672(3)	<i>Si</i> –O(5)	1.643(3)
<i>Ca</i> –O(4)	2.425(3)	< <i>Si</i> –O>	1.643
<i>Ca</i> –O(5)	2.399(3)		
<i>Ca</i> –O(5)	2.552(3)		
< <i>Ca</i> –O>	2.454		
<i>M</i> (1)–O(1) x2	1.840(2)	<i>M</i> (2)–O(1) x2	1.875(2)
<i>M</i> (1)–O(2) x2	1.963(3)	<i>M</i> (2)–O(3) x2	2.009(2)
<i>M</i> (1)–O(5) x2	1.979(3)	<i>M</i> (2)–O(4) x2	1.988(3)
< <i>M</i> (1)–O>	1.927	< <i>M</i> (2)–O>	1.957

TABLE 7. Refined site-scattering values and assigned site-populations.

Site	Refined site-scattering (epfu)	Assigned site-population (apfu)	Calculated site-scattering (epfu)	Mean cation radius (\AA)
<i>M</i> (1)	9.79	0.19 Al + 0.30 Ti + 0.01 Ta	9.80	0.579
<i>M</i> (2)	19.36	0.084 Al + 0.162 Ti + 0.144 Ta + 0.09 Nb + 0.02 Fe	19.38	0.611
<i>Ca</i>	20.00	1.00 Ca	20.00	

epfu – electrons per formula unit

(2005) in a synthetic titanite-like material $\text{Ca}(\text{Ti}_x\text{Zr}_{1-x})\text{GeO}_4\text{O}$ with Zr for Ti substitution >0.7 apfu. A triclinic structure was found in two titanite samples from the Hefsetjern pegmatite, Tørdal, southern Norway, enriched in Ta + Nb, Sn, Al + Fe^{3+} and some REE (Lussier *et al.*, 2009).

Żabińskiite is isostructural with triclinic titanite (Lussier *et al.*, 2009) and is bond-topologically identical with titanite and other minerals of the titanite group. The refined site-scattering values show that the heavy cations Ta^{5+} and Nb^{5+} are almost completely ordered at the *M*(2) site. The

TABLE 8. Powder pattern for žabińskiite.

<i>I</i>	<i>d</i> (calc) (Å)	<i>h</i>	<i>k</i>	<i>l</i>	<i>I</i>	<i>d</i> (calc) (Å)	<i>h</i>	<i>k</i>	<i>l</i>
11	6.432	1	0	0	5	1.971	$\bar{3}$	$\bar{2}$	2
65	4.939	0	1	1	13	1.950	0	1	3
	—	0	$\bar{1}$	1		—	0	$\bar{1}$	3
15	4.745	$\bar{1}$	$\bar{1}$	1	5	1.815	$\bar{3}$	$\bar{3}$	1
10	4.346	0	2	0		—	$\bar{1}$	4	2
9	3.606	$\bar{1}$	2	0	10	1.804	$\bar{1}$	$\bar{4}$	2
	—	1	2	0		—	$\bar{2}$	4	0
11	3.407	1	$\bar{1}$	1	10	1.797	2	4	0
	—	1	1	1	6	1.762	3	1	1
100	3.226	$\bar{2}$	$\bar{1}$	1		—	0	4	2
98	3.001	0	0	2		—	0	$\bar{4}$	2
89	2.609	0	3	1	18	1.740	$\bar{1}$	3	3
	—	0	$\bar{3}$	1		—	$\bar{4}$	0	2
6	2.591	$\bar{2}$	2	0	13	1.732	$\bar{2}$	4	2
8	2.383	$\bar{2}$	2	2	13	1.720	2	4	2
	—	1	0	2		—	$\bar{2}$	3	3
12	2.360	2	$\bar{1}$	1	31	1.704	4	1	1
	—	2	1	1		—	2	$\bar{1}$	2
20	2.283	1	$\bar{3}$	1		—	$\bar{2}$	2	2
	—	1	3	1		—	4	$\bar{1}$	1
11	2.257	$\bar{3}$	1	1	3	1.669	0	5	1
	—	$\bar{3}$	$\bar{1}$	1		—	0	5	$\bar{1}$
3	2.220	$\bar{2}$	$\bar{3}$	1	23	1.645	0	3	3
	—	$\bar{3}$	0	2		—	0	3	$\bar{3}$
6	2.173	0	4	0	7	1.608	4	$\bar{2}$	2
11	2.113	$\bar{1}$	1	3		—	4	0	0
	—	$\bar{1}$	$\bar{1}$	3	11	1.559	3	0	4
10	2.085	1	2	2		—	$\bar{2}$	5	1
	—	1	$\bar{2}$	2	10	1.551	$\bar{2}$	$\bar{5}$	1
29	2.063	$\bar{2}$	$\bar{1}$	3		—	$\bar{3}$	$\bar{4}$	2
	—	$\bar{1}$	4	0					

resultant difference in constituent-cation radii at the two sites (Table 7) is 0.032 Å, in close accord with the corresponding difference in mean bond length (Table 6) of 0.030 Å. Lussier *et al.* (2009) discussed the case of (Al,Ta,Nb)-bearing titanite, indicating that if the substitution $(\text{Al,Fe})^{3+} + (\text{Ta,Nb})^{5+} \rightarrow 2\text{Ti}^{4+}$ is significant at the *Y* site of the titanite structure, “the Al + Ta arrangement propagates along the chain direction to produce the sequence ...Al–Ta–Al–Ta–Al–Ta... which will eventually produce the structural sequence ...*M*(1)–*M*(2)–*M*(1)–*M*(2)–*M*(1)–*M*(2) ... which breaks the monoclinic symmetry to produce triclinic titanite”, and furthermore “...the case ... suggests that only substitution $(\text{Al, Fe})^{3+} + (\text{Ta,Nb})^{5+} \rightarrow 2\text{Ti}^{4+}$ will give rise to triclinic $A\bar{1}$ titanite at ambient conditions” (*ibidem*, p. 718). Žabińskiite is a sample of such a titanite-group

species containing ~64 mol.% $\text{Ca}[\text{Al}_{0.5}(\text{Ta,Nb})_{0.5}]\text{SiO}_4\text{O}$, i.e. considering data for synthetic aluminioan-tantalian titanite (Liferovich and Mitchell, 2006a), almost completely saturated in that component. However, synthetic, high-temperature $\text{Ca}(\text{Ti}_{0.4}\text{Al}_{0.3}\text{Ta}_{0.3})\text{SiO}_4\text{O}$ has the monoclinic $A2/a$ structure, not the triclinic $A\bar{1}$ structure. We can only agree with Lussier *et al.* (2009) that for (Al,Ta,Nb)-bearing titanite and žabińskiite, the monoclinic–triclinic transition is induced not by composition but temperature. Both titanites studied by Lussier *et al.* (2009) and also (Al,Ta,Nb)-bearing titanite and žabińskiite from Piława Górna originate from pegmatites and crystallized at relatively low temperature close to the appearance of a fluid phase, whereas Liferovich and Mitchell (2006a) synthesized their $\text{Ca}(\text{Ti}_{0.4}\text{Al}_{0.3}\text{Ta}_{0.3})\text{SiO}_4\text{O}$

compound at 1225–1175°C. Thus, żabińskiite may be a natural proof that low-temperature crystallization produces the triclinic species with Ta and Nb completely ordered at the *M*(2) site, and high-temperature crystallization results in a disordered monoclinic arrangement.

Origin

To date, the highest contents of Ta and Nb have been measured in two titanites that occur as tiny inclusions in (Ta,Nb)-rich rutile from the Craveggia pegmatite, Italy (Prior and Zambonini, 1908; Clark,

1974) and the Maršíkov pegmatite, Czech Republic (Černý *et al.*, 1995); the titanites contain 16.0 wt.% Ta₂O₅ + 2.9 wt.% Nb₂O₅ and 21.5 wt.% Ta₂O₅ + 9.5 wt.% Nb₂O₅, respectively. The origin of the Maršíkov titanite is related to the interaction of metamorphic pore fluids, generated mainly by dehydration reactions, with Nb-Ta oxides and components of silicate host rocks. The highly variable composition of this titanite is explained as a result of low mobility of the solute reactants, heterogeneity of the fluid phase, and a lack of post-crystallization equilibration (Černý *et al.*, 1995). The origin of the Craveggia titanite is explained by crystallization under conditions that facilitate Ta

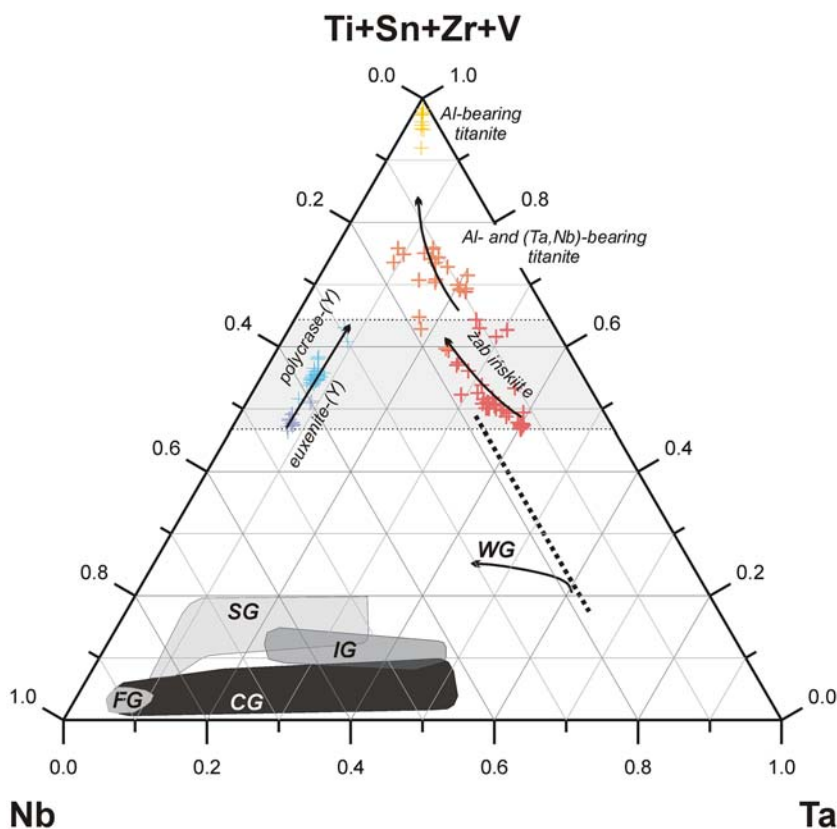


FIG. 7. Position of żabińskiite in the crystallization sequences of (Fe,Mn)-(Ti,Sn)-(Nb,Ta) and (Y,REE,U,Th)-Ti-(Nb,Ta) oxides in the Piława Górna pegmatitic system (Piecza *et al.*, 2013, 2014; Szuszkiewicz *et al.*, 2015). The lightest-grey section of the triangle marks the Nb-Ta-Ti range in which żabińskiite crystallized coevally with polycrase-(Y) and euxenite-(Y). Abbreviations: CG – columbite-group minerals; IG – ixiolite-group minerals; SG – samarskite-group minerals; FG – fergusonite-group minerals; WG – wodginite-group minerals. Symbols: black solid arrows – evolution trends in the titanite-group minerals and coexisting euxenite-group minerals, and in the wodginite-group minerals; dotted line – a threshold of 20 at.% of Nb, which constitutes the border separating żabińskiite and Al- and (Ta,Nb)-bearing titanite from (Nb,Ta)-bearing oxides.

and Nb partitioning between the titanite and rutile structures in (Ta,Nb)-rich environments (Paul *et al.*, 1981). Titanite with moderate (Nb,Ta)-enrichment is also found as a late constituent of miarolitic cavities, e.g. in the Huron claim pegmatite (Paul *et al.*, 1981) and the Irgon claim pegmatite (Groat *et al.*, 1985), SW Manitoba, Canada, and in the Heftejern pegmatite in Norway (Lussier *et al.*, 2009).

Żabińskiite, the (Ta,Al)-analogue of titanite, was found in a weakly- to moderately- fractionated NYF-affiliated part of the hybrid NYF + LCT Piława Górna pegmatitic system as fracture fillings in a cracked crystal of zircon intergrown with euxenite-(Y) and polycrase-(Y); rutile is absent from this assemblage. The Piława Górna pegmatites formed from a granitic anatectic melt with the important role of magmatic fractionation, generated from a metasedimentary-metavolcanic protolith during amphibolite-facies retrogressive metamorphism ~381–377 Ma (*cf.* Szuszkiewicz *et al.*, 2013; Pieczka *et al.*, 2015c; Turniak *et al.*, 2015). During solidification, the late-stage melt became enriched in Ca, Fe, Sn, Sc and Ti and a fluid phase rich in Ca and Ta exsolved. This change in composition resulted in a distinct reversal Mn-Fe fractionation as recorded by the Fe(Mn)-Ti(Sn)-(Nb,Ta) oxides (Pieczka *et al.*, 2013). Late-stage enrichment in Ca is also reflected by the replacement of spessartine garnet by Ca-bearing

spessartine, progressive Ca-enrichment of ishikawaite, samarskite-(Y) and polycrase-(Y) and their subsequent alteration to Ca-bearing pyrochlore-supergrupp minerals (Pieczka *et al.*, 2014; Szuszkiewicz *et al.*, 2015), crystallization of titanite- and epidote-group minerals in fracture-controlled vein-like alteration zones in blocky feldspar, crystallization of fersmite, late Ca-enrichment of Cs-rich beryl and pezzottaite (Pieczka *et al.*, 2016), alteration of beryl to various members of the bavenite-bohseite series (Szeleg *et al.*, 2017) and the increasing role of Ca during the crystallization of REE-bearing mineral assemblages composed of Ca-free keiviite-(Y), Ca-enriched gadolinite-(Y), Ca-bearing hingganite-(Y), pilawite-(Y), hellandite-(Y), allanite-(Y), epidote and zoisite (Pieczka *et al.*, 2015a). Żabińskiite and (Al,Ta,Nb)-bearing titanite crystallized during a probably short-term episode of increasing Ti and Nb and simultaneous decreasing Ta and Ta + Nb (Figs 7, 8). The episode corresponds closely with crystallization of accompanying polycrase-(Y) and euxenite-(Y) that required similar geochemical conditions (Szuszkiewicz *et al.*, 2015). Tantalum was preferentially incorporated into żabińskiite, Nb into the euxenite-group minerals, and Ti was incorporated by all these phases. In the Piława Górna pegmatites, euxenite-group minerals occur mainly as patches along feldspar-quartz boundaries and probably crystallized in a very narrow time interval from a

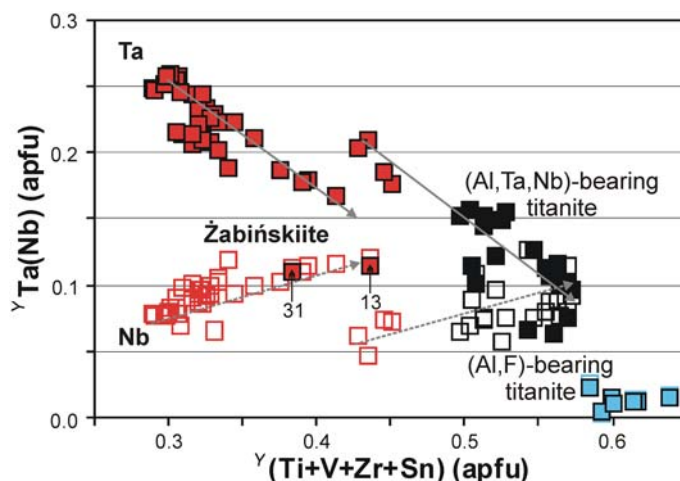


FIG. 8. Nb and Ta fractionation trends in żabińskiite (red), (Al,Ta,Nb)-bearing titanite (black) and (Al,F)-bearing titanite (blue). Symbols: empty squares – Nb; full squares – Ta; dotted grey arrows – trends of Nb fractionation; continuous grey arrows – trends of Ta fractionation. The analyses 13 and 31 with Ta < Nb (Table 2) are marked by short, black vertical arrows (detailed explanation in the text).

flux-rich melt and/or fluid phase with the Mn/(Mn+Fe) ratio approaching 0.50, increasing Ca and decreasing Ta/(Nb + Ta) and Ti (Szuszkiewicz *et al.*, 2015). Comparing the values of Ta/(Nb + Ta) in (Al,Ta,Nb)-dominant żabińskiite (0.49–0.82), (Al,Ta,Nb)-bearing titanite (0.35–0.72) and (Al,F)-bearing titanite (0.43–0.56), it seems likely that żabińskiite (at least partly) could have also crystallized simultaneously or nearly simultaneously with ferrowodginitite [Ta/(Nb + Ta) = 0.61–0.75] and samarskite-group minerals at high Ca, Al and Ti activities (*cf.* Pieczka *et al.*, 2013, 2014). We suggest that titanite-group minerals in the żabińskiite-bearing pegmatite crystallized in the following order: (1) żabińskiite at relatively high Ti and Ta activities, (2) (Al,Ta,Nb)-bearing titanite marking the decrease in the Ta and Ta + Nb activities, (3) (Al,F)-bearing titanite marking the increasing activity of volatiles, mainly H₂O. Slightly elevated contents of fluorine in the Al-enriched titanite is probably a result of its preferential partitioning into the structure of such titanite because there is no evidence for a significant increase of the activity of F in other minerals (e.g. micas) in the investigated pegmatite. On the contrary, all weakly to moderately evolved NYF-affiliated Piława Górna pegmatites are poor in F (Szuszkiewicz *et al.*, 2013).

Fine-scale compositional zoning commonly observed in żabińskiite and associated (Al,Ta,Nb)-bearing titanite is most likely the effect of relatively slow diffusion of quadrivalent and pentavalent cations (*cf.* Brady and Cherniak, 2010), and indicate that both minerals crystallized from environments that were geochemically inhomogeneous on the local scale. Although żabińskiite and (Al,Ta,Nb)-bearing titanite show similar concentrations of Nb that increase slightly from ~0.04 to ~0.12 apfu with fractionation, they show highly heterogeneous patchy distribution of Ta that oscillates from ~0.31 to ~0.16 apfu in various domains of (Al,Ta,Nb)-bearing żabińskiite and from ~0.21 to ~0.17 apfu in different regions of Ti-bearing żabińskiite, grading to (Al,Ta,Nb)-bearing titanite (Fig. 8). Irregular patchy domains of (Al,F)-bearing titanite within the mosaic żabińskiite and (Al,Ta,Nb)-bearing titanite (Fig. 1d) can be considered as a product of exsolution due to limited miscibility between (Al,Ta,Nb)-bearing titanites, including żabińskiite and (Al,F)-bearing titanite (Cempírek *et al.*, 2008 and discussion therein).

The exotic composition of żabińskiite expressed by high contents of Ta and Ta + Nb as well as Al, Ti

and Ca suggests that the conditions required for its crystallization may be restricted to NYF-affiliated pegmatites of the rare-element class that had some amounts of Ti and Ca added, probably from an external source. In such systems, żabińskiite might be expected to crystallize at the stage when the Ta/(Ta + Nb) fractionation index exceeds 0.50 in Fe (Mn)-Ti(Sn)-(Ta,Nb) oxides, and is close to 0.50–0.40 in (REE,Ca,U,Th)-(Ti,Nb,Ta) oxides of the samarskite and euxenite groups. High, but decreasing activity of Ta and simultaneously increasing activity of Ti (Fig. 8) seems to be rather time-restricted during the geochemical evolution of the pegmatite because the amounts of these two elements in the pegmatite-forming melt are mostly controlled by crystallization of such minerals as titanite, polycrase-(Y) and euxenite-(Y).

Two out of 70 analyses of titanite-group minerals from the Piława Górna pegmatite show $2 \cdot (\text{Nb} + \text{Ta}) > \text{Ti}$, with Nb slightly exceeding Ta, suggesting the possible existence of a Nb-analogue of żabińskiite, $\text{Ca}(\text{Al}_{0.5}\text{Nb}_{0.5})(\text{SiO}_4)\text{O}$. However, both analyses also show the presence of some $\text{Na}(\text{Ta,Nb})(\text{SiO}_4)\text{O}$ and $\text{Ca}(\text{Ta,Nb})(\text{AlO}_4)\text{O}$ compounds and, therefore, although the compounds with Nb > Ta prevail, the dominance of the $\text{Ca}(\text{Al}_{0.5}\text{Nb}_{0.5})(\text{SiO}_4)\text{O}$ end-member is ambiguous. Taking into account the relationships between $^{\text{Y}}\text{Ta}$, $^{\text{Y}}\text{Nb}$ and $^{\text{Y}}\text{Ti}$ in the Ta–Nb–Ti–Al–Si system (Fig. 8), the conditions required for the crystallization of Nb-dominant analogue of żabińskiite would be even more restricted than the ones necessary for the formation of żabińskiite-like compositions and even (Al,Ta,Nb)-bearing titanite that crystallized after żabińskiite and contains more Ta than Nb. It seems that Nb-dominant compositions observed in these two analyses could be achieved only at a distinct $^{\text{Y}}\text{Al}$ excess, manifested by elevated contents of the $\text{CaAl}(\text{SiO}_4)(\text{F,OH})$ compound. In fact, both analyses are Ta-depleted, probably due to the substitution $0.5\text{Al}^{3+} + (\text{F,OH})^- \rightarrow 0.5\text{Ta}^{5+} + \text{O}^{2-}$. Concluding, we regard that the crystallization of a Nb-analogue of żabińskiite in nature is highly unlikely.

Acknowledgements

We thank members of the IMA CNMNC, Peter Leverett, Ray Macdonald, Pavel Uher and Peter Williams (Principal Editor) for their comments on this manuscript. The studies were supported by the National Science Centre (Poland) grant 2015/19/B/ST10/01809 to AP, and by a Canada Research Chair in Crystallography and Mineralogy, by a Natural

Sciences and Engineering Research Council of Canada Discovery grant, and by Innovation grants from the Canada Foundation for Innovation to FCH, and by the National Science Foundation (NSF) grant EAR-1322082 to GRR. SEM-EBSD analysis was carried out at the Caltech GPS Division Analytical Facility, which is supported, in part, by NSF grants EAR-0318518 and DMR-0080065.

References

- Aftalion, M. and Bowes, D.R. (2002) U–Pb zircon isotopic evidence for Mid–Devonian migmatite formation in the Gory Sowie domain of the Bohemian Massif, Sudeten Mountains, SW Poland. *Neues Jahrbuch für Mineralogie, Monatshefte*, **4**, 182–192.
- Alexander, J.B. and Flinter, B.H. (1965) A note on varlamoffite and associated minerals from the Batang Padang district, Perak, Malaya, Malaysia. *Mineralogical Magazine*, **35**, 622–627.
- Bartelmehs, K.L., Bloss, F.D., Downs, R.T. and Birch, J.B. (1992) EXCALIBUR II. *Zeitschrift für Kristallographie*, **199**, 185–196.
- Basso, R., Lucchetti, G., Zefiro, L. and Palenzona, A. (1994) Vanadomalayaite, CaVOSiO_4 , a new mineral vanadium analog of titanite and malayaite. *Neues Jahrbuch für Mineralogie Monatshefte*, 489–498.
- Beirau, T., Mihailova, B., Malcherek, T., Paulmann, C., Bismayer, U. and Groat, L.A. (2014) Temperature-induced $P2_1/c$ to $C2/c$ phase transition in partially amorphous (metamict) titanite revealed by Raman spectroscopy. *The Canadian Mineralogist*, **52**, 91–100.
- Bernau, R. and Franz, G. (1987) Crystal chemistry and genesis of Nb-, V-, and Al-rich metamorphic titanite from Egypt and Greece. *The Canadian Mineralogist*, **25**, 695–705.
- Bismayer, U., Schmahl, W., Schmidt, C. and Groat, L.A. (1992) Linear birefringence and X-ray diffraction studies of the structural phase transition in titanite, CaTiSiO_5 . *Physics and Chemistry of Minerals*, **19**, 260–266.
- Brady, J.B. and Cherniak, D.J. (2010) Diffusion in minerals: An overview of published experimental diffusion data. Pp. 899–920 in: *Diffusion in Minerals and Melts* (Y. Zhang and D.J. Cherniak, editors). Reviews in Mineralogy & Geochemistry, **72**. Mineralogical Society of America, Chantilly, Virginia, USA.
- Bröcker, M., Żelaźniewicz, A. and Enders, M. (1998) Rb–Sr and U–Pb geochronology of migmatitic gneisses from the Góry Sowie (West Sudetes, Poland): the importance of Mid–Late Devonian metamorphism. *Journal of the Geological Society, London*, **155**, 1025–1036.
- Brueckner, H.K., Blusztajn, J. and Bakun-Czubarow, N. (1996) Trace element and Sm–Nd “age” zoning in garnets from peridotites of the Caledonian and Variscan mountains and tectonic implications. *Journal of Metamorphic Geology*, **14**, 61–73.
- Cempírek, J., Houzar, S. and Novák, M. (2008) Complexly zoned niobian titanite from hedenbergite skarn at Písek, Czech Republic, constrained by substitution $\text{Al}(\text{Nb,Ta})\text{Ti}_{2-2}$, $\text{Al}(\text{F,OH})(\text{TiO})_{-1}$ and SnTi_{-1} . *Mineralogical Magazine*, **72**, 1293–1305.
- Černý, P. and Riva di Sanseverino, L. (1972) Comments on crystal chemistry of titanite. *Neues Jahrbuch für Mineralogie Monatshefte*, 97–103.
- Černý, P., Novák, M. and Chapman, R. (1995) The $\text{Al}(\text{Nb,Ta})\text{Ti}_{2-2}$ substitution in titanite: the emergence of a new species? *Mineralogy and Petrology*, **52**, 61–73.
- Chakhmouradian, A.R. (2004) Crystal chemistry and paragenesis of compositionally-unique (Al-, Fe-, Nb-, and Zr-rich) titanite from Afrikanda, Russia. *American Mineralogist*, **89**, 1752–1762.
- Chakhmouradian, A.R. and Zaitsev, A.N. (2002) Calcite-amphibole-clinopyroxene rock from Afrikanda Complex, Kola peninsula, Russia: mineralogy and possible link to carbonatites. III. Silicate minerals. *The Canadian Mineralogist*, **40**, 1347–1374.
- Chakhmouradian, A.R., Reguir, E.P. and Mitchell, R.H. (2003) Titanite in carbonatitic rocks: Genetic dualism and geochemical significance. *Periodico di Mineralogia*, **72**, Eurocarb Special Issue, 107–113.
- Clark, A.M. (1974) A tantalum-rich variety of sphene. *Mineralogical Magazine*, **39**, 605–607.
- Della Ventura, G., Bellatreccia, F. and Williams, C.T. (1999) Zr- and LREE-rich titanite from Tre Croci, Vico volcanic complex (Latinum, Italy). *Mineralogical Magazine*, **63**, 123–130.
- Ellemann-Olesen, R. and Malcherek, T. (2005) Temperature and composition dependence of structural phase transition in $\text{Ca}(\text{Ti}_x\text{Zr}_{1-x})\text{OGeO}_4$. *American Mineralogist*, **90**, 687–694.
- Gaines, R.V., Skinner, H.C., Foord, E.E., Mason, B. and Rosenzweig, A. (1997) *Dana's New Mineralogy*. Eighth Edition, John Wiley & Sons, Inc, USA.
- Gordon, S.M., Schneider, D.A., Manecki, M. and Holm, D.K. (2005) Exhumation and metamorphism of an ultrahigh-grade terrane: geochronometric investigations of the Sudetes Mountains (Bohemia), Poland and Czech Republic. *Journal of the Geological Society, London*, **162**, 841–855.
- Groat, L.A., Carter, R.T., Hawthorne, F.C. and Ercit, T.S. (1985) Tantalian niobian titanite from Irgon claim, southeastern Manitoba. *The Canadian Mineralogist*, **23**, 569–571.
- Hatert, F. and Burke, E.A.J. (2008) The IMA–CNMNC dominant-constituent rule revisited and extended. *The Canadian Mineralogist*, **46**, 717–728.
- Hawthorne, F.C., Ungaretti, L. and Oberti, R. (1995) Site populations in minerals: terminology and presentation of results of crystal-structure refinement. *The Canadian Mineralogist*, **33**, 907–911.

- Higgins, J.B. and Ribbe, P.H. (1976) The crystal chemistry and space group of natural and synthetic titanites. *American Mineralogist*, **61**, 878–888.
- Higgins, J.B. and Ribbe, P.H. (1977) The structure of malayaite, CaSnOSiO_4 , a tin analog of titanite. *American Mineralogist*, **62**, 801–806.
- Hollabaugh, C.L. and Foit, Jr., F.F. (1984) The crystal structure of an Al-rich titanite from Grisons, Switzerland. *American Mineralogist*, **69**, 725–732.
- Houzar, S., Litochleb, J., Sejkora, J., Cempírek, J. and Cícha, J. (2008) Unusual mineralization with niobian titanite and Bi-tellurides in scheelite skarn from Kamenné doly quarry near Písek, Moldanubian Zone, Bohemian Massif. *Journal of Geosciences*, **53**, 1–16.
- Kek, S., Aroyo, M., Bismayer, U., Schmidt, C., Eichhorn, K. and Krane, H.G. (1997) The two-step phase transition of titanite, CaTiSiO_5 : a synchrotron radiation study. *Zeitschrift für Kristallographie*, **212**, 9–19.
- Kryza, R. (1981) Migmatization in gneisses of the northern part of the Sowie Góry, Sudetes. *Geologia Sudecka*, **16**, 7–91 [in Polish, English summary].
- Kryza, R. and Fanning, C.M. (2007) Devonian deep-crustal metamorphism and exhumation in the Variscan Orogen: evidence from SHRIMP zircon ages from the HT–HP granulites and migmatites of the Góry Sowie (Polish Sudetes). *Geodinamica Acta*, **20**, 159–176.
- Liferovich, R.P. and Mitchell, R.H. (2006a) Tantalum-bearing titanite: synthesis and crystal structure data. *Physics and Chemistry of Minerals*, **33**, 73–83.
- Liferovich, R.P. and Mitchell, R.H. (2006b) Crystal structure of a synthetic aluminous tantalum titanite: a reconnaissance study. *Mineralogical Magazine*, **70**, 115–121.
- Lussier, A.J., Cooper, M.A., Hawthorne, F.C. and Kristiansen, R. (2009) Triclinic titanite from the Hefetjern granitic pegmatite, Tørdal, Southern Norway. *Mineralogical Magazine*, **73**, 709–722.
- Ma, C. and Rossman, G.R. (2008) Barioperovskite, BaTiO_3 , a new mineral from the Benitoite Mine, California. *American Mineralogist*, **93**, 154–157.
- Ma, C. and Rossman, G.R. (2009) Tistarite, Ti_2O_3 , a new refractory mineral from the Allende meteorite. *American Mineralogist*, **94**, 841–844.
- Markl, G. and Piazzolo, S. (1999) Stability of high-Al titanite from low-pressure calcsilicates in light of fluid and host-rock composition. *American Mineralogist*, **84**, 37–47.
- Mazur, S., Aleksandrowski, P., Kryza, R. and Obercdziedzic, T. (2006) The Variscan orogen in Poland. *Geological Quarterly*, **50**, 89–118.
- Meyer, H.W., Zhang, M., Bismayer, U., Salje, E.K.H., Schmidt, C., Kek, S., Morgenroth, W. and Bleser, T. (1996) Phase transformation of natural titanite: an infrared, Raman spectroscopic, optical birefringence and X-ray diffraction study. *Phase Transitions*, **59**, 39–60.
- O'Brien, P.J., Kröner, A., Jaeckel, P., Hegner, E., Żelaźniewicz, A. and Kryza, R. (1997) Petrological and isotope studies on Palaeozoic high-pressure granulites. Góry Sowie Mts, Polish Sudetes. *Journal of Petrology*, **38**, 433–456.
- Paul, B.J., Černý, P., Chapman, R. and Hinthorne, J.R. (1981) Niobian titanite from the Huron Claim pegmatite, southeastern Manitoba. *The Canadian Mineralogist*, **19**, 549–552.
- Pieczka, A., Szuszkiewicz, A., Szełęg, E., Nejbert, K., Łodziński, M., Ilnicki, S., Turniak, K., Banach, M., Hołub, W., Michałowski, P. and Różniak, R. (2013) (Fe,Mn)–(Ti,Sn)–(Nb,Ta) oxide assemblage in a little fractionated portion of a mixed (NYF + LCT) pegmatite from Piława Górna, the Sowie Mts. block, SW Poland. *Journal of Geosciences*, **58**, 91–112.
- Pieczka, A., Szuszkiewicz, A., Szełęg, E., Ilnicki, S., Nejbert, K. and Turniak, K. (2014) Samarskite-group minerals and alteration products: an example from the Julianna pegmatitic system, Piława Górna, SW Poland. *The Canadian Mineralogist*, **52**, 303–319.
- Pieczka, A., Hawthorne, F.C., Cooper, M., Szełęg, E., Szuszkiewicz, A., Turniak, K., Nejbert, K. and Ilnicki, S. (2015a) Pilawite-(Y), $\text{Ca}_2(\text{Y,Yb})_2[\text{Al}_4(\text{SiO}_4)_4\text{O}_2(\text{OH})_2]$, a new mineral from the Piława Górna granitic pegmatite, southwestern Poland: mineralogical data, crystal structure and association. *Mineralogical Magazine*, **79**, 1143–1157.
- Pieczka, A., Hawthorne, F.C., Ma, C., Rossman, G.R., Buffat, P., Rutkowski, B., Szełęg, E., Szuszkiewicz, A., Turniak, K., Nejbert, K. and Ilnicki, S.S. (2015b) Żabińskiite, IMA 2015-033. CNMNC Newsletter No. 26, August 2015, page 945; *Mineralogical Magazine*, **79**, 941–947.
- Pieczka, A., Szuszkiewicz, A., Szełęg, E., Janeczek, J. and Nejbert, K. (2015c) Granitic pegmatites of the Polish part of the Sudetes (NE Bohemian massif, SW Poland). *7th International Symposium on Granitic Pegmatites, Książ, Poland, June 17–19, 2015*. Fieldtrip Guidebook, C, 73–103.
- Pieczka, A., Szełęg, E., Szuszkiewicz, A., Gołębiowska, B., Zelek, S., Ilnicki, S., Nejbert, K. and Turniak, K. (2016) Cs-bearing beryl evolving to pezzottaite from the Julianna pegmatitic system, SW Poland. *The Canadian Mineralogist*, **54**, 115–124.
- Pouchou, I. L. and Pichoir, F. (1985) “PAP” (phi-rho-z) procedure for improved quantitative microanalysis. Pp. 104–106 in: *Microbeam Analysis* (J.T. Armstrong, editor). San Francisco Press, San Francisco, California, USA.
- Prior, G.T. and Zambonini, F. (1908) On strüverite and its relation to ilmenorutile. *Mineralogical Magazine*, **15**, 78–89.

- Rath, S., Kunz, M. and Miletich, R. (2003) Pressure-induced phase transition in malayaite, CaSnOSiO_4 . *American Mineralogist*, **88**, 293–300.
- Russell, J.K., Groat, L.A. and Halleran, A.A.D. (1994) LREE-rich niobian titanite from Mount Bisson, British Columbia: chemistry and exchange mechanisms. *The Canadian Mineralogist*, **32**, 575–587.
- Sahama, Th.G. (1946) On the chemistry of mineral titanite. *Bulletin de la Commission Géologique de Finlande*, **24**(138), 88–120.
- Sawka, W.N., Campbell, R.B. and Norrish, K. (1984) Light-rare-earth-element zoning in sphene and allanite during granitoid fractionation. *Geology*, **12**, 131–134.
- Sheldrick, G.M. (2000) *SHELXTL Version 6.14*. Bruker Analytical X-ray Systems, Inc., Madison, Wisconsin, USA.
- Sheldrick, G.M. (2008) A short history of SHELX. *Acta Crystallographica*, **A64**, 112–122.
- Speer, J.A. and Gibbs, G.V. (1976) The crystal structure of synthetic titanite, CaTiOSiO_4 , and the domain textures of natural titanites. *American Mineralogist*, **61**, 238–247.
- Stepanov, A.V., Bekenova, G.K., Levin, V.L. and Hawthorne, F.C. (2012) Natrotitanite, ideally $(\text{Na}_{0.5}\text{Y}_{0.5})\text{Ti}(\text{SiO}_4)\text{O}$, a new mineral from the Verkhnēe Espe deposit, Akjailyautas mountains, Eastern Kazakhstan district, Kazakhstan: description and crystal structure. *Mineralogical Magazine*, **76**, 39–44.
- Strunz, H. and Nickel, E.H. (2001) *Strunz Mineralogical Tables, Ninth Edition*. Schweizerbart'sche Verlagsbuchhandlung, Stuttgart, Germany.
- Szeleg, E., Zuzens, B., Hawthorne, F.C., Pieczka, A., Szuszkiewicz, A., Turniak, K., Nejbert, K., Ilnicki, S., Friis, H., Makovicky, E., Weller, M.T. and Lemée-Cailleau, M.H. (2017) Bohseite, ideally $\text{Ca}_4\text{Be}_4\text{Si}_9\text{O}_{24}(\text{OH})_4$, from the Piława Górna quarry, the Góry Sowie Block, SW Poland. *Mineralogical Magazine*, **81**, 35–46.
- Szuszkiewicz, A., Szeleg, E., Pieczka, A., Ilnicki, S., Nejbert, K., Turniak, K., Banach, M., Łodziński, M., Różniak, R. and Michałowski, P. (2013) The Julianna pegmatite vein system at the Piława Górna mine, Góry Sowie Block, SW Poland – preliminary data on geology and descriptive mineralogy. *Geological Quarterly*, **57**, 467–484.
- Szuszkiewicz, A., Pieczka, A., Szeleg, E., Ilnicki, S., Nejbert, K. and Turniak, K. (2015) Mineral chemistry of euxenite-group minerals from the Julianna pegmatites, Piława Górna, Sudetes, SW Poland. *7th International Symposium on Granitic Pegmatites, PEG 2015 Książ, Poland*. Book of Abstracts, 107–108.
- Taylor, M. and Brown, G.E. (1976) High-temperature structural study of the $P2_1/a \leftrightarrow A2/a$ phase transition in synthetic titanite, CaTiSiO_5 . *American Mineralogist*, **61**, 435–447.
- Tiepolo, M., Oberti, R. and Vanucci, R. (2002) Trace-element incorporation in titanite: constraints from experimentally determined solid/liquid partition coefficients. *Chemical Geology*, **191**, 105–119.
- Timmermann, H., Parrish, R.R., Noble, S.R. and Kryza, R. (2000) New U–Pb monazite and zircon data from the Sudetes Mountains in SW Poland: evidence for a single-cycle Variscan orogeny. *Journal of the Geological Society, London*, **157**, 265–268.
- Turniak, K., Pieczka, A., Kennedy, A.K., Szeleg, E., Ilnicki, S., Nejbert, K. and Szuszkiewicz, A. (2015) Crystallisation age of the Julianna pegmatite system (Góry Sowie Block, NE margin of the Bohemian massif): evidence from U–Th–Pb SHRIMP monazite and CHIME uraninite studies. *7th International Symposium on Granitic Pegmatites, PEG 2015 Książ, Poland*. Book of Abstracts, 111–112.
- Uher, P., Černý, P., Chapman, R., Határ, J. and Miko, O. (1998) Evolution of Nb,Ta-oxide minerals in the Prašivá granitic pegmatites, Slovakia. II. External hydrothermal Pb,Sb overprint. *The Canadian Mineralogist*, **36**, 535–545.
- Van Breemen, O., Bowes, D.R., Aftalion, M. and Żelaźniewicz, A. (1988) Devonian tectonothermal activity in the Sowie Góry gneissic block, Sudetes, southwestern Poland: evidence from Rb–Sr and U–Pb isotopic studies. *Journal of the Polish Geological Society*, **58**, 3–10.
- Woolley, A.R., Platt, R.G. and Eby, N. (1992) Niobian titanite from the Ilomba nepheline syenite complex, north Malawi. *Mineralogical Magazine*, **56**, 428–430.
- Żelaźniewicz, A. (1990) Deformation and metamorphism in the Góry Sowie gneiss complex, Sudetes, SW Poland. *Neues Jahrbuch für Geologie und Paläontologie, Abhandlungen*, **179**, 129–157.
- Zhang, M., Salje, E.K.H., Bismayer, U., Unruh, H.-G., Wruck, B. and Schmidt, C. (1995) Phase transition(s) in titanite CaTiSiO_5 : an infrared spectroscopic, dielectric response and heat capacity study. *Physics and Chemistry of Minerals*, **22**, 41–49.